

Modern Physics Letters A
© World Scientific Publishing Company

LOW-MASS DIFFRACTION AT THE LHC

L.L. JENKOVSKY

*Bogolyubov Institute for Theoretical Physics (BITP) of the
National Academy of Sciences of Ukraine,
14-b, Metrolohichna str., Kiev, 03680, Ukraine
jenk@bitp.kiev.ua*

O.E. KUPRASH

*Faculty of Physics, Taras Shevchenko National University,
2, Glushkova ave., Kiev, 03022, Ukraine
oleg.kuprash@desy.de*

J.W. LÄMSÄ

*Physics Department, Iowa State University,
Ames, 50011 Iowa, USA
jerry.lamsa@cern.ch*

R. ORAVA

*Division of Elementary Particle Physics, Helsinki Institute of Physics,
P.O. Box 64 (Gustaf Hällströminkatu 2a), F1-00014 University of Helsinki, Finland;
CERN, CH-1211 Geneva 23, Switzerland
rorava@cc.helsinki.fi; risto.orava@cern.ch*

Received 30.06.2011
Revised (Day Month Year)

The expected resonance structure for the low-mass single diffractive states from a Regge-dual model elaborated paper by the present authors in a previous is predicted. Estimates for the observable low-mass single diffraction dissociation (SDD) cross sections and efficiencies for single diffractive events simulated by PYTHIA 6.2 as a function of the diffractive mass are given.

Keywords: Diffraction Dissociation; LHC; CMS

PACS Nos.: 11.55.-m, 11.55.Jy, 12.40.Nn

1. Single Diffraction Dissociation (SDD)

Low-mass single diffraction dissociation (SDD) will be among the first measurements at the LHC ¹. While high-mass diffractive scattering ^{2 3 4 5} receives much attention - mainly due to its relatively straightforward interpretation through triple Regge formalism and successful measurements at the ISR, HERA and Tevatron - the low-mass SD still lacks both experimental measurement and theoretical understanding.

2 *L. Jenkovszky, O. Kuprash, J. Lamsa, and R. Orava*

The unpolarized elastic pp differential cross section is given by ⁶

$$\frac{d\sigma}{dt} = \frac{[3\beta F^p(t)]^4}{4\pi \sin^2[\pi\alpha_P(t)/2]} (s/s_0)^{2\alpha_P(t)-2}, \quad (1)$$

where the constant β is obtained by normalizing $d\sigma/dt \approx 80$ mb/GeV² at $t = 0$. The linear Pomeron trajectory is $\alpha(t) = 1.08 + 0.25t$; the increase with energy is provided by the supercritical Pomeron intercept. A dipole form can be used for the form factor ^{7 8}

$$F_1^p(t) = \frac{4m^2 - 2.9t}{4m^2 - t} \frac{1}{(1 - t/0.71)^2}, \quad (2)$$

where m denotes the proton mass. Assuming Regge factorization, the double differential cross section for single diffractive scattering (SD)

$$pp \rightarrow pX, \quad (3)$$

can be written as ^{7 8}

$$\frac{d^2\sigma}{dt dM^2} \sim \frac{9\beta^4 [F_1^p(t)]^2}{4\pi \sin^2[\pi\alpha_P(t)]} (s/M^2)^{2\alpha_P(t)-2} \left[\frac{W_2}{2m} \left(1 - M^2/s\right) - mW_1(t + 2m^2)/s^2 \right], \quad (4)$$

where W_i , $i = 1, 2$ are related to the structure functions of the nucleon, and $W_2 \gg W_1$. At high M^2 , the W s are Regge-behaved, while at small M^2 their behavior is dominated by nucleon resonances N^* s. Thus, the behavior of (4) in the low missing mass region largely depends on the transition form factors or resonance structure functions, typically $\gamma^*p \rightarrow N^* \rightarrow \pi p$. The knowledge of the inelastic form factors (or transition amplitudes) is crucial for the calculation of low-mass diffraction dissociation (3) by using equation (4). The transition amplitudes (inelastic form factors) were introduced in Ref. ⁶. We use a supercritical Pomeron, with the intercept $\alpha_P(0) \approx 1.1$ and slope 0.2 GeV⁻². At the LHC energies, terms M^2/s and $(t + 2m^2)/s^2$ can be safely neglected in Eq. (4). Furthermore, the signature factor in the amplitude $\frac{1 - e^{-i\pi\alpha_P(t)}}{\sin\pi\alpha_P(t)}$, used in Refs. ^{7 8} is replaced by an exponential (see Ref. ¹) $e^{-i\pi\alpha_P(t)/2}$. For the elastic proton form factor, $F^p(t)$, a dipole form

$$F_1^p(t) = \frac{1}{(1 - t/0.71)^2}, \quad (5)$$

is used.

At the LHC energies, Eq. (4) now simplified as

$$\frac{d^2\sigma}{dt dM_X^2} \approx \frac{9\beta^4 [F^p(t)]^2}{4\pi} (s/M_X^2)^{2\alpha_P(t)-2} \frac{W_2}{2m}. \quad (6)$$

In Fig. 1 double differential cross sections are shown for two c.m.s. energies, $\sqrt{s} = 7$ and 14 TeV with different values of the four-momentum squared, t .

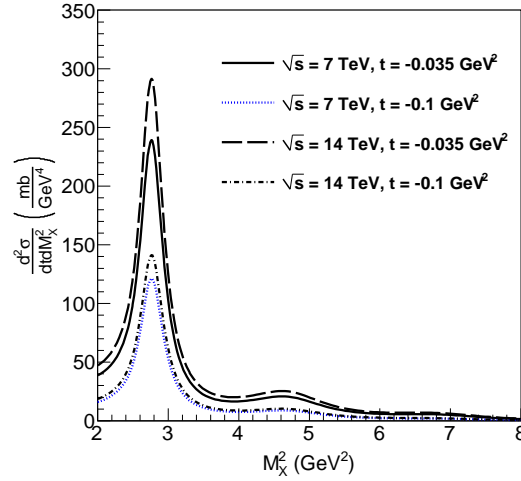


Fig. 1. Cross section calculated for the single diffraction dissociation (SD) by using Eq. (4) for the LHC energies $\sqrt{s} = 7$ and 14 TeV for different values of the four-momentum transfer, $-t = (p-p')^2$. For details see Ref. ⁵.

2. Forward detectors and efficiencies at the LHC

In the following, an analysis of acceptance effects is carried out for a predicted observed spectrum of low-mass SD cross section. The forward detector lay-out of the CMS experiment is used in calculations. Somewhat similar results can be obtained by the ATLAS experiment ¹. At the CMS intersect, IP5, the TOTEM T1 and T2

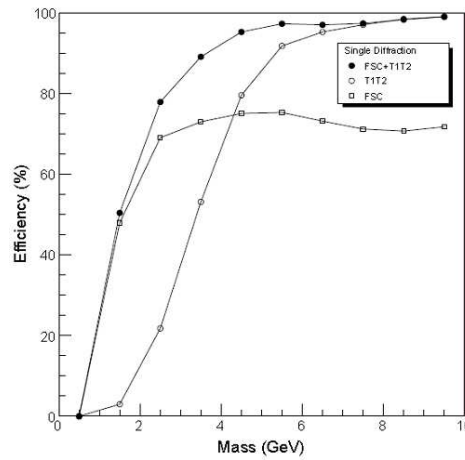


Fig. 2. The calculated efficiencies for single diffractive events simulated by PYTHIA 6.2 as a function of the diffractive mass. Five charged particles (hits) are required in any of the FSC, or at least one track in the η region covered by T1 or T2.

4 *L. Jenkovszky, O. Kuprash, J. Lämsä, and R. Orava*

trackers can be employed to detect SD masses below $M_X = 10$ GeV (see Fig. 2 and Ref. ¹). The total η regions spanned by T1 and T2 is, approximately $3 < |\eta| < 7$. The combination of T1 and T2, labeled the *T1T2* veto, can be used to reject any event having a charged track in the T1T2 eta region. At the ATLAS intersect, IP1, a similar η region is, in principle, covered by the forward calorimetry and LUCID luminosity detector.

Forward Shower Counters, FSC, can be added closely surrounding the beam pipes, at $60 \text{ m} < |z| < 85 \text{ m}$ (between the MBXW elements of D1), and at further locations out to $z = \pm 140 \text{ m}$ on both sides of the interaction point, IP5 (or similarly the experimental areas of ALICE, ATLAS or LHCb), see Ref. ⁹.

The trigger efficiencies of the forward detector systems ^a ¹ for single-diffractive interactions, as a function of the diffractive mass, simulated by PYTHIA and the GEANT program sequence are shown in Figure 2.

Three trigger possibilities for data collection are considered. The first would be to trigger on events without any restriction (minimum bias), i.e., *no veto*. The second would be a trigger with a veto on a given eta range, i.e., a T1T2 veto. The third would be a combination of T1T2 + FSC veto.

3. Model calculations

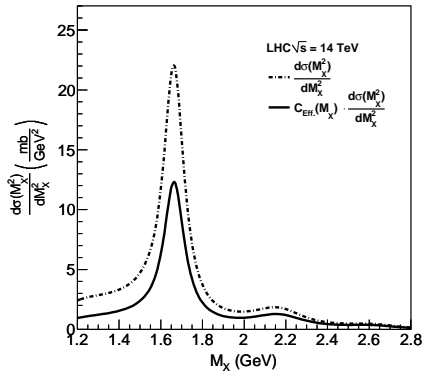


Fig. 3. Differential cross section $d\sigma/dM_X^2$, corrected for CMS detectors acceptance.

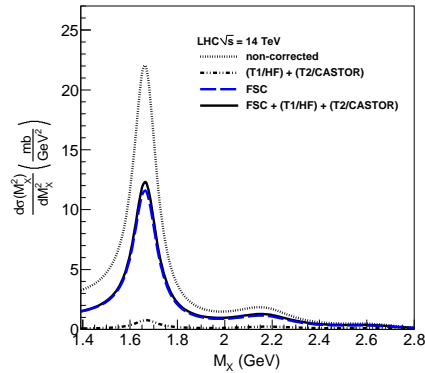


Fig. 4. Same as on the left panel, but for different detector combinations

In Figures 3-6, the model calculations for the low mass SD process (Eq. 6, Fig. 1) are corrected by the experimental efficiencies (Fig. 2). The forward detector systems T1 and T2 (or equivalently the HF and CASTOR calorimeters) facilitate detection of forward diffractive masses down to about 4 GeV, far above the three dominating N^* states.

^aIn our analysis we use the forward detector system of the CMS/TOTEM experiment.

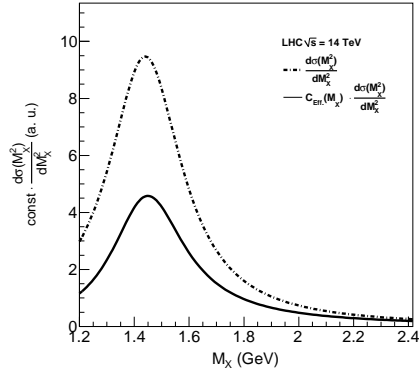


Fig. 5. Roper resonance signal, corrected for CMS detectors acceptance (arbitrary units).

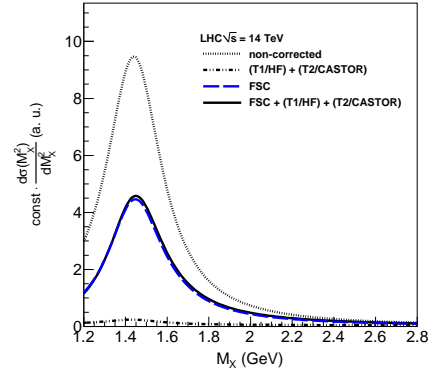


Fig. 6. Same as on the left panel, but for different detector combinations (arbitrary units).

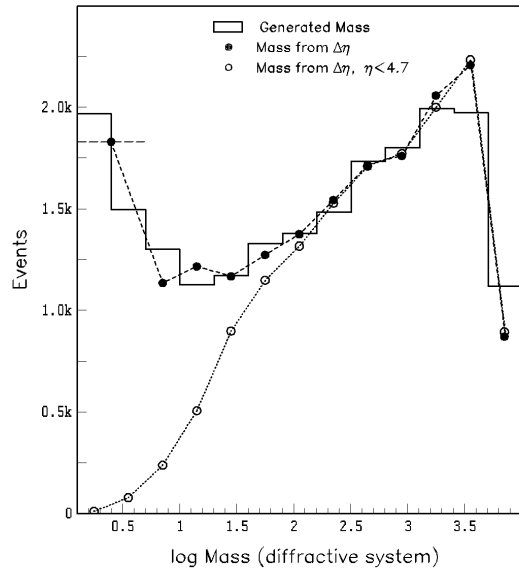


Fig. 7. Generated diffractive mass and reconstructed diffractive mass calculated for two cases of detector coverage

An approximate calculation of the diffractive mass can be made through its relation to the size of the rapidity gap adjacent to the scattered proton. The adjacent rapidity gap is defined as the gap between the diffractive proton (close to the beam rapidity) and the nearest particle in rapidity. The correspondence between the diffractive mass M and the pseudorapidity gap $\Delta\eta$ is $M_X/\sqrt{s} \sim e^{\Delta\eta}$.

To provide a more precise (although model dependent) measurement, the

6 *L. Jenkovszky, O. Kuprash, J. Lamsa, and R. Orava*

PYTHIA program has been used to determine the correlation between the diffractive mass and the size of the rapidity gap. Figure 7 shows the actual (generated) diffractive mass together with that calculated by the above method, for two cases: (a) for full eta coverage, and (b) for limited eta range $|\eta| < 4.7$, i.e., the nominal CMS coverage.

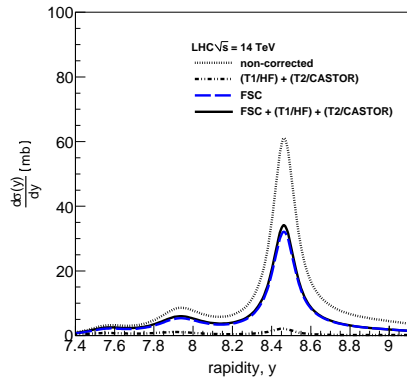


Fig. 8. Differential cross section $d\sigma/dy$, corrected for CMS detectors acceptance (rapidity $y = -\ln \frac{M_X^2}{m_p \sqrt{s}}$).

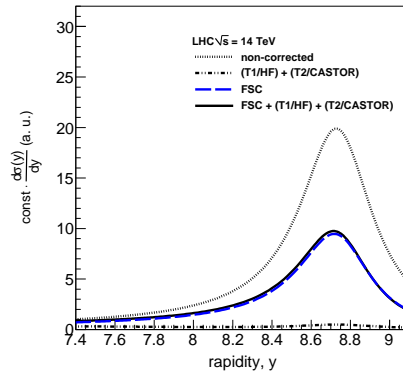


Fig. 9. Roper resonance signal as function of rapidity, corrected for CMS detectors acceptance (arbitrary units).

The efficiency of the Forward Shower Counters for detecting forward diffractive systems is high. For low-mass single diffraction one relies largely on the FSC's. Measurement of the content (off-line) of individual FSC counters, which cover different eta-ranges, provides more differential tests of the diffractive event simulation. From the various rates, with knowledge of the FSC efficiencies, the background contributions can be estimated and subtracted from different situations (e.g., different M_X). Correlations between the FSC counters can be determined and compared with expectations. These will be used to make more precise determinations of the mass of the diffractive system. The ultimate uncertainties to be achieved will come from work which is still in progress. Another valuable check will be the independence of all the measured cross sections on the instantaneous luminosity.

In the model presented here, there is no significant contribution from the so called Roper resonance, $N^*(1440)$. For completeness, the case where the $N^*(1440)$ dominates the low SD masses was considered. This mass region would be efficiently covered by the additional Forward Shower Counters (see Fig.4, fsc references), and x of the $N^*(1440)$ final states would be covered.

4. Conclusions

The low mass single diffractive (SD) processes remain largely unknown at current collider energies. In this paper model calculations together with simulated experi-

mental efficiencies are presented for the single diffractive proton-proton events below $M_x = 10$ GeV. The N^* states $N^*(1675, 1680, \dots)$ MeV dominate the low mass region and do not allow simple $1/M_X^2$ extrapolations to be used for estimating the event rates missed by the base line experiments.

As further steps comparison of the event rates and uncertainties below $M_X = 10$ GeV should be made, including:

- $1/M_X^2$ extrapolation to 1 GeV vs. the N^* spectrum calculation,
- uncertainties in these.

Although low-mass diffraction at the ISR and Tevatron energies was studied in quite a number of papers, the details of the complicated resonance structure in the missing mass at the LHC energies still leaves quite a number of open problems. For example, the slope of the diffraction cone is known to increase monotonically as the missing mass increases beyond the resonance region, see, e.g. Fig. 19 of Ref. ⁴, this may not be the case in the resonance region, scrutinized in the present paper, see Fig 1. A behavior of the local slope (as function of the missing mass and t) in the resonance region may affect considerably the efficiency of the forward shower counters. A complementary means to study low-mass diffraction are finite-energy mass rules (FMSR), relating low- and high-missing mass dynamics (see Ref. ⁵). It should be remembered, however, that FMSR contain information only on the average, i.e. the integrated behavior of the resonant amplitude, without providing details about separate resonances contributions. Moreover, the resonance contribution in the FMSR integral should be appended by an independent elastic contribution and a vaguely known background, see Ref. ¹⁰. We intend to come back to these interesting and important problems in a future study.

On the basis of our model calculations, the three dominating N^* states remain below the detection thresholds of the current forward detectors at the LHC. By installing Forward Shower Counters (see Refs. above), the rates of these small mass diffractive events can be recorded thus facilitating an accurate measurement of the total pp cross section at the LHC.

Acknowledgements

We thank V. Magas for discussions and K. Goulios for useful correspondence. RO gratefully acknowledges the Academy of Finland for support. O.K. is grateful to Rainer Schicker and the EU program “Diffractive and Electromagnetic Processes at the LHC” for their support. L.J. was supported by the Project “Matter under Extreme Conditions” of the Nat. Ac. Sc. of Ukraine, Dept. of Astronomy and Physics.

8 *L. Jenkovszky, O. Kuprash, J. Lämsä, and R. Orava*

References

1. R. Fiore, L. Jenkovszky, R. Orava, E. Predazzi, A. Prokudin, O. Selyugin, *Forward Physics at the LHC; Elastic Scattering*, Int. J. Mod. Phys., A24: 2551 (2009), arXiv:hep-ph/0812.0539.
2. D.P. Roy and R.G. Roberts, Nucl. Phys. B **77** (1974) 240.
3. A.B. Kaidalov, Phys. Rep. **50** (1979) 157.
4. K. Goulianos, Phys. Rep. **101** (1983) 169.
5. K. Goulianos and J. Montanha, Phys. Rev. **D59** (1999) 114017, hep-ph/9805496.
6. L. Jenkovszky, O. Kuprash, J. Lämsä, V. Magas, and R. Orava, *Dual-Regge approach to high-energy, low-mass diffraction dissociation*, Phys. Rev. D 83, 056014 (2011), arXiv:hep-ph/1011.0664
7. G.A. Jaroszkiewicz and P.V. Landshoff, Phys. Rev. **10** (1974) 170.
8. A. Donnachie, P.V. Landshoff, Nucl. Phys. B **244** (1984) 322.
9. V. A. Khoze, J.W. Lämsä, R. Orava and M.G. Ryskin, *Forward Physics at the LHC, Detecting Elastic pp Scattering by Radiative Photons*, hep-ph/1007.3721.
10. L. Jenkovszky, O. Kuprash, and V. Magas, *Low-mass diffraction at the LHC; role of the background*, in the Proceedings of "Diffraction-2010", Otranto, 2010.